INTERNATIONAL JOURNAL FOR NUMERICAL AND ANALYTICAL METHODS IN GEOMECHANICS, VOL. 20, 403–430 (1996)

HYDRATION SWELLING OF WATER-ABSORBING ROCKS: A CONSTITUTIVE MODEL

WOLFGANG K. HEIDUG

Shell Research Rijswijk, Volmerlaan 8, 2288 GD Rijswijk, The Netherlands

SAU-WAI WONG

Sarawak Shell Bhd, Miri, Malayasia

SUMMARY

Water-absorbing rocks are formed from minerals that can hold water in their crystal structure or between grain boundaries. Such water absorption is often accompanied by a change in the crystal dimension that manifests itself as a swelling of the rock. Swelling is particularly pronounced in rocks containing phyllosilicates because of the ease with which these minerals hydrate; it is thus of geological and geotechnical relevance in shales, clay-rich soils and zeolitized tuffs. The model of hydration swelling that we present here is based on extended versions of the equations of poroelasticity and Darcy's transport law, which we derive using a non-equilibrium thermodynamics approach. Our equations account for the hydration reaction under the assumption that the reaction rate is fast in comparison with the rate at which hydraulic state changes are communicated through the rock, i.e. that local physico-chemical equilibrium persists. Using a finite-element scheme for solving numerically the governing equations of our model, we simulate the creep of shales during a routine swelling test and calculate the stress and strain distributions around wellbores drilled in shale formations that undergo swelling. We show that swelling effects promote tensile failure of the wellbore wall.

KEY WORDS: swelling; chemo-poroelasticity; borehole stability; osmosis

1. INTRODUCTION

Swelling phenomena in rocks result from the change in crystal dimension or grain boundary width that arises when water is incorporated into the crystal structure or absorbed onto grain boundaries. Swelling is particularly pronounced in rocks containing minerals of the phyllosilicate class, whose crystal structure consists of stacked silicate layers (Reference 1, Chapter 15). When a phyllosilicate crystal is put in contact with water, hydration and electrical forces become operative between the silicate layers. The latter forces have their origin in the charging of silica surfaces exposed to water (e.g. Reference 2, Chapter 6), and the former forces result from the ordering of polar water molecules near hydrated solid surfaces (Reference 3, Chapter 13.5). Both kinds of forces are repulsive and hence have the capability to disjoin the stacked silicate layers, thereby causing swelling. Experimental evidence indicates, however, that the swelling of rocks in the upper earth crust is mainly due to hydration forces (References 1, Chapter 10; 4 and 5), as electrical forces are typically too weak to overcome the compressive force of the overburden.

CCC 0363–9061/96/060403–28

Received 21 April 1995
Revised 1 November 1995

Rock deformation caused by swelling is of widespread geomechanical relevance and of interest in disparate areas of the earth sciences. It is of concern to the civil engineer because of the often severe structural damage caused by expansive soils;[6,7,2] the geologist cannot afford to neglect swelling in the context of assessing the suitability of formations to serve as waste repositories;[8,9] swelling is a problem for the drilling engineer, as it may threaten the stability of wells drilled through shales with high phyllosilicate content.[10–12]

Despite its practical relevance, few attempts seem to have been made to develop a comprehensive constitutive description of swelling at the macroscopic scale. A macroscopic approach that is guided by the general principles of continuum thermomechanics seeks to derive the general structure of the constitutive equations for water-absorbing rocks from the general principles of macrolevel physics without delving into the microscopic physico-chemical basis of swelling. The precise form the constitutive equations take for specific mineral/fluid combinations, i.e. the determination of the material-dependent parameters, is left either to experimental work or taken from dedicated studies involving microstructural considerations.

A main advantage of such a macroscopic approach to the formulation of constitutive equations is its simplicity in comparison to a method that involves formulating constitutive equations first at the microscale and then scaling them up to the macroscale. This scaling-up procedure was followed, for example, by Heidug[13] to develop constitutive equations for a rock that undergoes phase reactions with the pore fluid. When adapted to accommodate hydration reactions, this procedure leads to the same results obtained here but through a more circuitous route.

At the macroscale a fluid-infiltrated rock can be viewed in two fundamentally different ways: either as a *heterogenous mixture* of a solid and fluid phase or as a *single continuum* with, however, effective solid/fluid properties. This difference in perception expresses itself in the constitutive description. A mixture-type description maintains the individuality of the solid and fluid phase and formulates constitutive equations for each phase separately, taking due account of phase interaction effects. This point of view has been advanced in work by Hueckel,[14] Karalis,[15] Mow *et al.*[16] and Snijders *et al.*[17] (the latter two papers dealing not with the swelling of rocks but with the related phenomenon of the swelling of biological tissues). All these authors have adopted the general theory of interacting continua (e.g. Reference 18) to develop constitutive equations. The problem with the mixture approach, however, is that it relies on information on the interaction between the phases that is difficult to obtain, and this lack of information must very often be filled by physical intuition and *ad hoc* assumptions. In addition, the rather detailed description of the constitutive response that this approach provides is often beyond what is needed for practical purposes and what can be possibly validated by experiments.

For that reason we shall adopt here a perspective that does not explicitly discriminate between the solid and the fluid phase but views a fluid-infiltrated rock as a single continuum. This is, of course, the view taken in Biot's[19] classical theory of poroelasticity, whose concern is the constitutive response of small volume elements of rock material filled with fluid when there is no physico-chemical interaction between fluid and rock matrix. In developing our theory and thereby extending Biot poroelasticity to account for hydration swelling effects we shall rely extensively on arguments from non-equilibrium thermodynamics. This ensures, in particular, the consistency of our theory with the second law of thermodynamics, a feature that sets our model apart from related work.[20]

The following discussion substantially enhances and complements that given by Wong and Heidug.[21] It is based on a balance equation for the Helmholtz free energy of a fluid-infiltrated rock that we find from combining the first and second law of thermodynamics. By specifying in the balance statement an entropy production term, we obtain the extension of Biot's equations and Darcy's flow law that incorporate physico-chemical interaction effects. A key assumption in our

argument is that the mineral matrix undergoes only elastic deformations and that the hydration reaction is fast in comparison to the time with which hydraulic changes are communicated through the rock, i.e. local physico-chemical equilibrium is maintained. Complementing our equations with a diffusion equation for the transport of solute, we arrive at a complete set of equations specifying the linear constitutive response of water-absorbing rocks to mechanical and chemical loading.

The complex nature of the governing equations of our theory prevents us from obtaining solutions for the stress–strain response analytically. So we have taken recourse to finite-element-based numerical methods to get some quantitative results. Specifically, we use our model to analyse an experiment on the linear flow of a salt solution through a shale sample and the swelling of the sample that accompanies the flow. Finding good qualitative agreement with observations, we proceed to extend the finite-element solution scheme to accommodate radial flow geometry and to analyse the evolution of stress and strain near a wellbore when drilling fluid is lost to the formation and physico-chemical interaction processes between drilling fluid and formation rock are active.

2. BALANCE LAWS

The foundation upon which we base the following discussion is the balance equation for the Helmholtz free energy. Under isothermal conditions this quantity becomes identical to the rock's strain energy and consequently holds the key to the formulation of constitutive equations.

Let R denote an arbitrary macroscopic region within the rock. We envision the boundary ∂R of R to be attached to the solid phase, so that the evolution of ∂R in space is determined exclusively by the motion of the solid matrix. Thus, no *solid* matter crosses the boundary ∂R as the rock deforms, and the mass content of region R can change only through the influx and efflux of *fluid* matter. In the jargon of thermodynamics, region R constitutes a system that is *open* with respect to the exchange of fluid mass but *closed* with respect to the exchange of solid mass.

The balance of Helmholtz free energy for the region R can be obtained by combining the statements of the first and the second law of thermodynamics for the matter contained in region R (as discussed in Appendix I). It reads

$$\left(\int_R \psi \, dv\right)^{\cdot} = -\int_{\partial R} \boldsymbol{\sigma}\mathbf{n}\cdot\mathbf{v}_s \, da - \int_{\partial R} \sum_k \mu^k \mathbf{I}^k \cdot \mathbf{n} \, da - T\int_{\partial R} \gamma \, dv \tag{1}$$

where the dot accent on the left-hand side indicates the material time derivative 'following' the motion of the solid. In equation (1) ψ is the density of the Helmholtz free energy, and $\boldsymbol{\sigma}$, $\mathbf{n}$, $\mathbf{v}_s$, T and γ, respectively, denote the Cauchy stress tensor, the outward unit normal vector, the velocity of the solid, the (constant) temperature and the entropy production per unit volume. The last, of course, by the dictates of the second law, is always non-negative. The symbols μ^k and $\mathbf{I}^k$ represent, respectively, chemical potential and the mass flux of the kth fluid component. More precisely, $\mathbf{I}^k$ is defined as

$$\mathbf{I}^k = \rho^k(\mathbf{v}^k - \mathbf{v}_s) \tag{2}$$

where $\mathbf{v}^k$ and ρ^k are, respectively, the velocity and the mass density of this fluid component.

Equation (1) states that the change in free energy of region R is the result of three processes, namely, the mechanical deformation of the boundary of R, the influx or efflux of fluid mass across ∂R, and the dissipation processes occurring within R. The terms in equation (1) that quantify these processes have a structure familiar to those well-acquainted with continuum mechanics and

thermodynamics. The first term on the right-hand side of equation (1) measures the integrated rate of work performed by the traction $\boldsymbol{\sigma}\mathbf{n}$ upon deforming an area element of the boundary that has velocity $\mathbf{v}_s$, while the second term quantifies the work expended per unit time to alter the masses of all the fluid components within region R.

Apart from the free energy, we shall also need to balance the partial masses contained in region R. For the solid mass, whose density we denote by ρ_s, one obviously has

$$\left(\int_R \rho_s \, dv\right)^{\cdot} = 0 \tag{3}$$

as there is no solid mass flux into region R. However, region R is open with respect to the exchange of fluid mass, so that

$$\left(\int_R \rho^k \, dv\right)^{\cdot} = -\int_{\partial R} \mathbf{I}^k \cdot \mathbf{n} \, da \tag{4}$$

Recognizing now the validity of equations (1)–(4) for any regular subregion of R and using Reynold's transport theorem, one obtains the localized version of the balance equation for the free energy

$$\dot{\psi} + \psi \operatorname{div} \mathbf{v}_s - \operatorname{div}(\boldsymbol{\sigma}\mathbf{v}_s) + \operatorname{div}\left(\sum_k \mu^k \mathbf{I}^k\right) = -T\gamma \leqslant 0 \tag{5}$$

together with that for the solid mass

$$\dot{\rho}_s + \rho_s \operatorname{div} \mathbf{v}_s = 0 \tag{6}$$

and the masses of the fluid component

$$\dot{\rho}^k + \rho^k \operatorname{div} \mathbf{v}_s + \operatorname{div} \mathbf{I}^k = 0 \tag{7}$$

The fluid component mass densities ρ^k appearing in the last equation are expressed relative to the unit volume of the fluid–solid mixture. They are related to the mass densities $\bar{\rho}^k$ these components possess intrinsically through

$$\rho^k/\phi = \bar{\rho}^k \tag{8}$$

where ϕ denotes the porosity.

The discussion so far assumed that the fluid is non-electrolytic, i.e. it does not contain any free ions. The extension of our results to pore fluids that are solutions of electrolytes is readily achieved using standard thermodynamic arguments (Reference 22, Section 8). It involves summing in the free energy balance equation (5) over all ionic species instead of the chemical components present in the pore fluid and replacing the chemical by the electro-chemical potentials. We recall that the electro-chemical potential $\tilde{\mu}^\alpha$ of the αth ionic species is related to this species' chemical potential μ^α through

$$\tilde{\mu}^\alpha = \mu^\alpha + z^\alpha \varphi \tag{9}$$

where z^α is the electrical charge of the αth ionic species and φ is the electrical potential, it being understood that the normalization of φ is such that this quantity vanishes at infinity in the absence of electrical charges. With these considerations, we find the local balance of free energy when the pore fluid contains ions as

$$\dot{\psi} + \psi \operatorname{div} \mathbf{v}_s - \operatorname{div}(\boldsymbol{\sigma}\mathbf{v}_s) + \operatorname{div}\left(\sum_\alpha \tilde{\mu}^\alpha \mathbf{I}^\alpha\right) = -T\gamma \leqslant 0 \tag{10}$$

3. ENTROPY PRODUCTION

Further progress now demands that we specify the dissipative processes operating within the rock, i.e. that we quantify the entropy production term γ in the balance law (5). We shall assume here that only one single dissipation mechanism is operative, namely the friction generated at the solid/fluid phase boundary when the fluid moves through the porous skeleton. By confining attention exclusively to solid/fluid friction, we exclude from consideration all dissipative processes related, in particular, to the inelastic deformation of the solid skeleton and to chemical reactions of the fluid components with one another and with the solid skeleton. Put differently, we assume that the solid undergoes only reversible elastic deformations and that all chemical species maintain a state of local chemical equilibrium. The latter requirement can be rephrased by recalling from classical thermodynamics that any unperturbed chemical system will evolve towards a state of equilibrium. Our chemical assumption can then be interpreted as a requirement for the rate with which the rock's state is perturbed by mechanical or chemical loading: these disturbances must occur with a characteristic time that is much larger than the time needed for any chemical reaction to relax towards equilibrium, i.e. external loading must be slower than internal chemical relaxation.

A macroscopic expression for the dissipation generated by the frictional resistance at the solid/fluid interface can be obtained either by averaging the microlevel flow field over representative volumes of rock material (e.g. Reference 23) or by using standard arguments of non-equilibrium thermodynamics (Reference 24, Section 10.4). Both routes lead to the same result, namely

$$0 \leqslant T\gamma = -\sum_k \mathbf{I}^k \cdot \operatorname{grad} \mu^k \tag{11}$$

This equation assumes a more convenient form if one replaces the fluxes $\mathbf{I}^k$, which measure the mass flow of component k relative to the solid matrix, by diffusion fluxes

$$\mathbf{J}^k = \rho^k(\mathbf{v}^k - \mathbf{v}_f) \tag{12}$$

that are relative to the mixture's barycentric velocity $\mathbf{v}_f = \sum_k (\rho^k/\rho_f)\mathbf{v}^k$, where $\rho_f = \sum_k \rho^k$ is the total fluid mass density. Obviously,

$$\mathbf{J}^k = \mathbf{I}^k - \rho^k(\mathbf{v}_f - \mathbf{v}_s) \tag{13}$$

Rearranging the terms of equation (13) so that it can be substituted into equation (11), we can rewrite the entropy production as

$$0 \leqslant T\gamma = -\mathbf{u} \cdot \operatorname{grad} p - \sum_k \mathbf{J}^k \cdot \operatorname{grad} \mu^k \tag{14}$$

Here we introduced the Darcy (filter) velocity through the definition

$$\mathbf{u} = \phi(\mathbf{v}_f - \mathbf{v}_s) \tag{15}$$

and made use of the Gibbs–Duhem equation in the fluid, which implies the identity

$$\sum_k \bar{\rho}^k \operatorname{grad} \mu^k = \operatorname{grad} p \tag{16}$$

the symbol p denoting the pore pressure.

As seen from their definition, the diffusion fluxes $\mathbf{J}^k$ are not all independent; they have to satisfy the constraint $\sum_k \mathbf{J}^k = 0$. Consequently, for a fluid comprising a solvent and a solute there

is only one independent diffusion flux, and the expression for the entropy production takes the form

$$0 \leqslant T\gamma = -\mathbf{u}\cdot\operatorname{grad} p - \mathbf{J}^{S}\cdot\operatorname{grad}(\mu^{S} - \mu^{D}) \tag{17}$$

in which the superscripts S and D refer to the solute and solvent (diluent), respectively.

The results that we have obtained so far apply for electrically neutral pore fluids. To extend them to pore fluids containing ions, i.e. solutions of electrolytes, we have to make the adaptations outlined at the end of the previous section, which involve replacing the chemical potentials by the electro-chemical ones. The expression for the entropy production now takes the form

$$0 \leqslant T\gamma = -\mathbf{u}\cdot\operatorname{grad} p - \sum_{\alpha} \mathbf{J}^{\alpha}\cdot\operatorname{grad}\tilde{\mu}^{\alpha} \tag{18}$$

which we can write as

$$0 \leqslant T\gamma = -\mathbf{u}\cdot\operatorname{grad} p - \sum_{\alpha} \mathbf{J}^{\alpha}\cdot\operatorname{grad}\mu^{\alpha} - \mathbf{i}\cdot\mathbf{E} \tag{19}$$

where $\mathbf{i} = \sum_{\alpha} z^{\alpha}\mathbf{J}^{\alpha}$ is an electrical conduction current and $\mathbf{E} = -\operatorname{grad}\varphi$ denotes the electrical field.

It is of considerable practical interest that the expression (19) for the entropy production in electrolytes be written in a form that is identical to equation (17) for neutral solute/solvent systems. This equivalence follows naturally from the assumption that one is dealing with a binary electrolyte, i.e. an electrolyte with two ionic species, and that the conduction current $\mathbf{i}$ is negligible (Reference 25, Section 4.18). A binary electrolyte contains four ionic species, namely water molecules, undissociated electrolyte molecules, cations and anions. We denote the chemical potential of the electrolyte molecules by μ^{S}, and by μ^{a} and μ^{c} the chemical potentials of the anions and cations, respectively. When dissociation equilibrium is reached, these quantities are related through the expression

$$\mu^{S} = \nu^{a}\mu^{a} + \nu^{c}\mu^{c} \tag{20}$$

in which the symbols ν^{a} and ν^{c}, respectively, indicate the numbers of anions and cations into which the parent electrolyte molecule dissociates. If $\mathbf{J}^{a}$ and $\mathbf{J}^{c}$ denote the respective mass fluxes of anions and cations, then the combinations $\mathbf{J}^{a}/\nu^{a}$ and $\mathbf{J}^{c}/\nu^{c}$ must be both equal to the flux of *dissociated* electrolyte molecules, as the solution has no net electrical charge. Denoting this flux by $\beta\mathbf{J}^{S}$, where β is the degree of dissociation, we have accordingly (Reference 25, Section 4.18)

$$\beta\mathbf{J}^{S} = (1/\nu^{a})\mathbf{J}^{a} = (1/\nu^{c})\mathbf{J}^{c} \tag{21}$$

Realizing that $(1-\beta)\mathbf{J}^{S}$ is the flux of undissociated electrolyte molecules, we can recast expression (19) for the entropy production as

$$0 \leqslant T\gamma = -\mathbf{u}\cdot\operatorname{grad} p - [(1-\beta)\mathbf{J}^{S}\cdot\operatorname{grad}\mu^{S} + \mathbf{J}^{a}\cdot\operatorname{grad}\mu^{a} + \mathbf{J}^{c}\cdot\operatorname{grad}\mu^{c} + \mathbf{J}^{D}\cdot\operatorname{grad}\mu^{D}] \tag{22}$$

This reduces to (17) upon keeping in mind that $\mathbf{J}^{S} + \mathbf{J}^{D} = \mathbf{0}$ and observing that by virtue of (20) and (21)

$$\mathbf{J}^{a}\cdot\operatorname{grad}\mu^{a} + \mathbf{J}^{c}\cdot\operatorname{grad}\mu^{c} = \beta\mathbf{J}^{S}\cdot\operatorname{grad}\mu^{S} \tag{23}$$

4. THE LINEAR TRANSPORT LAWS

To exploit equation (17) further, we write it in terms of the six-dimensional vectors $\mathscr{X}$ and $\mathscr{Y}$ defined by

$$\mathscr{X} = (-1/\bar{\rho}_{f})\operatorname{grad} p,\ -\operatorname{grad}(\mu^{S} - \mu^{D})),\quad \mathscr{Y} = (\bar{\rho}_{f}\mathbf{u}, \mathbf{J}^{S}) \tag{24}$$

According to equation (17), the scalar product of $\mathscr{X}$ with $\mathscr{Y}$ is always non-negative, $\mathscr{X} \cdot \mathscr{Y} \geqslant 0$. For non-trivial values of $\mathscr{X}$ and $\mathscr{Y}$ this can only hold if $\mathscr{X}$ and $\mathscr{Y}$ are functionally related. Assuming in the simplest case that this relation is linear, we conclude that

$$\bar{\rho}_f \mathbf{u} = -(L^{11}/\bar{\rho}_f) \operatorname{grad} p - L^{12} \operatorname{grad}(\mu^S - \mu^D) \tag{25}$$

$$\mathbf{J}^S = -(L^{21}/\bar{\rho}_f) \operatorname{grad} p - L^{22} \operatorname{grad}(\mu^S - \mu^D) \tag{26}$$

where the L^{ij} denote a set of phenomenological coefficients that are independent of grad p and grad $(\mu^S - \mu^D)$ but may very well depend on other parameters. The form in which we have stated equations (25) and (26) is appropriate for describing mass transport through *isotropic* media. For the general case of anisotropic flow, second-rank tensors $\mathbf{L}^{ij}$ would assume the role of the scalars L^{ij}.

A further simplification of our phenomenological equations could be achieved by assuming that the phenomenological coefficients in equations (25)–(26) satisfy Onsager's symmetry relation, which in the present case would stipulate that $L^{12} = L^{21}$. While Onsager symmetry is invariably invoked in the standard literature on the thermodynamics of irreversible processes,[26] the applicability to continuum thermodynamics of this principle is questioned in more recent work. In view of the dispute, it appears that the Onsager relation cannot claim the status of a *general* statement, even though it may be valid in particular situations. This view is supported by theoretical reasoning (Reference 27, Lecture 7) and by experimental results that show violations of Onsager symmetry (References 28 and 29, Section 15-1) for specific systems. For that reason we shall assume here L^{12} and L^{21} to be different coefficients and leave the last word on this matter to the experimentalist. (This independence of L^{12} and L^{21} allows us later to set $L^{21} = 0$ with impunity.)

For the further use of equations (25) and (26) it is convenient to have the chemical potentials replaced by the solute and diluent mass fractions defined, respectively, as

$$c^S = \bar{\rho}^S/\bar{\rho}_f = \rho^S/\rho_f, \quad c^D = \bar{\rho}^D/\bar{\rho}_f = \rho^D/\rho_f \tag{27}$$

where $\rho_f = \rho^S + \rho^D$ and $\bar{\rho}_f = \bar{\rho}^S + \bar{\rho}^D$. This is achieved with the help of the Gibbs–Duhem equation for the case of constant pressure, which states that

$$c^S(\mathrm{d}\mu^S)_p + c^D(\mathrm{d}\mu^D)_p = 0 \tag{28}$$

and also furnishes the expression

$$\operatorname{grad}(\mu^S - \mu^D) = (v^S - v^D) \operatorname{grad} p + \frac{1}{c^D} \frac{\partial \mu^S}{\partial c^S} \operatorname{grad} c^S \tag{29}$$

Here $v^S = \partial(1/\bar{\rho}^S)/\partial c^S$ and $v^D = \partial(1/\bar{\rho}^D)/\partial c^D$, respectively, denote the partial specific volumes of the solute and diluent, these quantities satisfying the thermodynamic identities

$$v^S = \frac{\partial \mu^S}{\partial p}, \quad v^D = \frac{\partial \mu^D}{\partial p} \tag{30}$$

Using relation (29) in equations (25) and (26) and assuming that $\bar{\rho}_f(v^S - v^D) \ll 1$, as is the case for a dilute solution, allows us to rewrite the transport equations as

$$\mathbf{u} = -\frac{k}{\nu}\left(\operatorname{grad} p - r \frac{\bar{\rho}_f}{c^D} \frac{\partial \mu^S}{\partial c^S} \operatorname{grad} c^S\right) \tag{31}$$

$$\mathbf{J}^S = -L\bar{\rho}_f \frac{\operatorname{grad} p}{p} - \bar{\rho}_f D \operatorname{grad} c^S \tag{32}$$

Here we introduced the permeability k through the definition

$$\frac{k}{\nu} = \frac{L^{11}}{\bar{\rho}_f^2} \tag{33}$$

in which ν denotes the fluid's viscosity, and the symbols r, L and D are given by

$$r = -\frac{L^{12}}{L^{11}}, \quad L = \frac{L^{21} p}{\bar{\rho}_f^2}, \quad D = \frac{L^{22}}{c^D \bar{\rho}_f} \frac{\partial \mu^S}{\partial c^S} \tag{34}$$

The latter two quantities can be regarded as a pressure diffusion coefficient and a dispersion-diffusion coefficient, respectively.

Equation (31) generalizes Darcy's law by recognizing that, in addition to the usual hydraulic gradient, gradients in the chemical composition of the pore fluid can act as a force that drives filtration. Such a force can occur when the porous structure is selective in its transport properties, i.e. it discriminates against (or favours) the transport of a specific component, as in the case of osmotic flow through semipermeable membranes. In fact, a transport equation of a form very similar to equation (31) has long been used in the biophysical and biochemical community to describe the transport of salt solutions through semipermeable biological membranes.[30,24] The quantity r, to which the literature sometimes refers as the reflection coefficient,[31] serves as a measure of the efficiency of the osmotic transport.

Equation (32) extends the usual form of the diffusion law, in which only concentration gradients act as driving forces, to account for the phenomenon of pressure diffusion, i.e. diffusion driven by pressure gradients (Reference 25, Section 4-23). However, to simplify the ensuing discussion, we shall assume that pressure diffusion effects are negligible, which amounts to requiring that

$$L = 0 \tag{35}$$

5. CONSTITUTIVE RELATIONS

Having discussed the mechanisms through which dissipation is generated, we are now in a position to extract from the balance equation for the free energy a fundamental equation of state and to formulate constitutive equations for the stress/strain response.

5.1. Equation of state

To this end, we use the expression for the entropy production (11) in the balance equation (5), assume that the rock maintains mechanical equilibrium as it deforms so that $\operatorname{div} \boldsymbol{\sigma} = 0$, and convert the resulting equation for ψ, namely

$$\dot{\psi} + \psi \operatorname{div} \mathbf{v}_s - \operatorname{tr}(\boldsymbol{\sigma} \operatorname{grad} \mathbf{v}_s) + \sum_k \mu^k \operatorname{div} \mathbf{I}^k = 0 \tag{36}$$

to a referential description. The last is necessary in order to introduce into our theory a measure of the rock's deformation state. We begin by recalling some concepts from continuum mechanics. Selecting an arbitrary reference configuration, we denote a place in it by $\mathbf{X}$. At time t this place occupies the position $\mathbf{x}$. The Green strain $\mathbf{E}$ is then defined in terms of the gradient $\mathbf{F}$ of the mapping $\mathbf{x}(\mathbf{X}, t)$, i.e.

$$\mathbf{F} = \frac{\partial \mathbf{x}}{\partial \mathbf{X}}(\mathbf{X}, t) \tag{37}$$

as

$$\mathbf{E} = \tfrac{1}{2}(\mathbf{F}^{\mathrm{T}}\mathbf{F} - \mathbf{1}) \tag{38}$$

This provides a measure of the rock's deformation state. In equation (38) we used the superscript T to indicate the transposed matrix, and we shall stick to this notation hereafter.

As a measure of the referential stress we introduce the second (symmetric) Piola–Kirchhoff stress T. This quantity is related to the Cauchy stress $\boldsymbol{\sigma}$ acting in the current configuration through

$$\mathbf{T} = J\mathbf{F}^{-1}\boldsymbol{\sigma}\mathbf{F}^{-\mathrm{T}}. \tag{39}$$

In this definition the symbol J denotes the determinant of the deformation gradient, $J = \det \mathbf{F}$. A glance at a continuum mechanics textbook reveals that it also admits the interpretation

$$J = \frac{\mathrm{d}V}{\mathrm{d}V_0} \tag{40}$$

where $\mathrm{d}V$ is the volume element in the current configuration that occupies volume $\mathrm{d}V_0$ in the reference configuration. Noting furthermore that the time derivative of J satisfies Euler's formula

$$\dot{J} = J \operatorname{div} \mathbf{v}_s \tag{41}$$

and observing the conservation equation (7) for the partial masses, we deduce from equation (36) that

$$\dot{\Psi} = \operatorname{tr}(\mathbf{T}\dot{\mathbf{E}}) + \sum_k \mu^k \dot{m}^k \tag{42}$$

This expression is the referential equivalent of equation (36). It relates the time change of the free energy $\Psi = J\psi$ per volume element in the reference configuration to the deformation rate $\dot{\mathbf{E}}$ and to the rate with which the mass $m^k = J\rho^k = J\phi\bar{\rho}^k$ of the kth component per unit referential volume changes in time.

The physical statement provided by equation (42) can be further sharpened by incorporating in it information about the thermodynamic state of the fluid. In water-absorbing rocks fluid can reside either in the space between individual clay platelets or in the pore space. Because of the narrow separation of the clay platelets, which is in the order of 10 Å, interstitial fluid is subject to intermolecular and surface forces[3] that cause the fluid's physical properties to deviate from those of the bulk. Water residing in the pores, however, does not feel the effect of these forces, as the pore dimensions are large in comparison to the distances over which the intermolecular forces are active. Accordingly, it obeys the familiar thermodynamic relations for bulk fluids. Denoting the Helmholtz free energy density of the pore water by ψ_f and is kth component's mass density per unit fluid volume by $\bar{\rho}^k_{\mathrm{pore}}$, we have from classical thermodynamics

$$\psi_f = -p + \sum_k \mu^k \bar{\rho}^k_{\mathrm{pore}} \tag{43}$$

and

$$\dot{\psi}_f = \sum_k \mu^k \dot{\bar{\rho}}^k_{\mathrm{pore}} \tag{44}$$

since according to the Gibbs–Duhem equation

$$\dot{p} = \sum_k \bar{\rho}^k \dot{\mu}^k \tag{45}$$

There is no *a priori* reason why the chemical potentials μ^k in the state equations (42) and (43) for the shale and the pore fluid should be equal. By postulating their equality, as we have done by

using the same symbol in both equations, we have tacitly invoked our earlier assumption concerning local chemical equilibrium. A difference in the chemical potentials is not consistent with this assumption, as it would act as a driving force for chemical equilibration processes.

To proceed further, we next calculate the free energy density of the 'wetted' mineral matrix, that is the free energy density of the mineral matrix inclusive of the fluid 'bound' between platelets. This quantity is obtained by subtracting from the free energy Ψ of the combined shale/fluid system the contribution $J\phi\psi_f$ due to the pore water. From equations (42)–(44) we find that this difference can be expressed as

$$(\Psi - J\phi\psi_f)^{\cdot} = \mathrm{tr}(\mathbf{T}\dot{\mathbf{E}}) + p\dot{v} + \sum_k \mu^k \dot{m}^k_{\text{bound}} \tag{46}$$

where

$$v = J\phi \tag{47}$$

denotes the pore volume per unit referential volume, and

$$m^k_{\text{bound}} = m^k - J\phi\bar{\rho}^k_{\text{pore}} \tag{48}$$

is the referential mass density of the kth fluid component in the bound water.

Instead of working directly with the potential $\Psi - J\phi\psi_f$, it is for our purposes more convenient to employ in the following the dual potential

$$W = (\Psi - J\phi\psi_f) - pv - \sum_k \mu^k m^k_{\text{bound}} \tag{49}$$

which we take as a function of $\mathbf{E}$, p and μ^k. Since equation (46) implies that the time derivative of $W(\mathbf{E}, p, \mu^k)$ satisfies the relation

$$\dot{W}(\mathbf{E}, p, \mu^k) = \mathrm{tr}(\mathbf{T}\dot{\mathbf{E}}) - v\dot{p} - \sum_k m^k_{\text{bound}}\,\dot{\mu}^k \tag{50}$$

we must have

$$\begin{gathered} T_{ij} = \left(\frac{\partial W}{\partial E_{ij}}\right)_{p,\mu^k}, \quad v = -\left(\frac{\partial W}{\partial p}\right)_{E_{ij},\mu^k} \\ m^k_{\text{bound}} = -\left(\frac{\partial W}{\partial \mu^k}\right)_{T_{ij},\mu^{l}(\neq \mu^k)} \end{gathered} \tag{51}$$

in order for equation (50) to be consistent with the expression for $\dot{W}$ obtained from the differentiation chain rule, namely

$$\dot{W} = \left(\frac{\partial W}{\partial E_{ij}}\right)_{p,\mu^k} \dot{E}_{ij} + \left(\frac{\partial W}{\partial p}\right)_{E_{ij},\mu^k} \dot{p} + \sum_k \left(\frac{\partial W}{\partial \mu^k}\right)_{E_{ij},p,\mu^{l}(\neq \mu^k)} \dot{\mu}^k \tag{52}$$

In writing equations (51) and (52) we referred the tensors $\mathbf{T}$ and $\mathbf{E}$ to a Cartesian co-ordinate system in which their components are T_{ij} and E_{ij}, $i, j = 1, 2, 3$. Upon differentiating equations (51) with respect to time, we obtain the following fundamental constitutive equations for the evolution of stress, pore volume fraction, and the mass densities in the bound water:

$$\dot{T}_{ij} = L_{ijkl}\dot{E}_{kl} - M_{ij}\dot{p} + \sum_k S^k_{ij}\dot{\mu}^k \tag{53}$$

$$\dot{v} = M_{ij}\dot{E}_{ij} + Q\dot{p} + \sum_k B^k\dot{\mu}^k \tag{54}$$

$$\dot{m}^k_{\text{bound}} = S^k_{ij}\dot{E}_{ij} + B^k\dot{p} + \sum_l Z^{kl}\dot{\mu}^l \tag{55}$$

Here the parameters L_{ijkl}, M_{ij}, S^k_{ij}, Q, B^k and Z^{kl} denote thermodynamic response coefficients that are defined through

$$L_{ijkl} = \left(\frac{\partial T_{ij}}{\partial E_{kl}}\right)_{p,\mu^k} = \left(\frac{\partial T_{kl}}{\partial E_{ij}}\right)_{p,\mu^k} \tag{56}$$

$$M_{ij} = -\left(\frac{\partial T_{ij}}{\partial p}\right)_{E_{ij},\mu^k} = \left(\frac{\partial v}{\partial E_{ij}}\right)_{p,\mu^k} \tag{57}$$

$$S^k_{ij} = \left(\frac{\partial T_{ij}}{\partial \mu^k}\right)_{E_{ij},p} = -\left(\frac{\partial m^k_{\text{bound}}}{\partial E_{ij}}\right)_{p,\mu^k} \tag{58}$$

$$Z^{kl} = \left(\frac{\partial m^k_{\text{bound}}}{\partial \mu^l}\right)_{E_{ij},p} = \left(\frac{\partial m^l_{\text{bound}}}{\partial \mu^k}\right)_{E_{ij},p} \tag{59}$$

$$B^k = \left(\frac{\partial v}{\partial \mu^k}\right)_{E_{ij},p} = \left(\frac{\partial m^k_{\text{bound}}}{\partial p}\right)_{E_{ij},\mu^k} \tag{60}$$

$$Q = \left(\frac{\partial v}{\partial p}\right)_{E_{ij},\mu^k} \tag{61}$$

The second definitions given in equations (56)–(60) derive from changing the order of differentiation after substituting equations (51) into the first definitions.

5.2. *Linear isotropic response*

The constitutive equations (53)–(55) are of rather general nature. We shall now simplify them through the procedure of physical and geometrical linearization.

The physical linearization of our constitutive equations involves the assumption that all the thermodynamic response coefficients L_{ijkl}, M_{ij}, S^k_{ij}, B^k, Q and Z^{kl}, which at this stage of the theoretical development are functions of the state parameters E_{ij}, p and μ^k, are material-dependent *constants*. With this stipulation the only source of non-linearity that remains in the constitutive laws is of geometrical nature and associated with the presence of large deformations. Upon requiring the strains to be small, we are justified (as discussed in detail in any continuum mechanics textbook) in replacing the Green strain tensor E_{ij} and the Piola–Kirchhoff stress T_{ij} by the infinitesimal strain tensor ε_{ij} of linear elasticity and the Cauchy stress σ_{ij}, respectively, i.e.

$$E_{ij} = \varepsilon_{ij}, \quad T_{ij} = \sigma_{ij} \tag{62}$$

The theory that emerges generalizes the classical theory of poroelasticity[19] by including the effects of pore fluid chemistry on the constitutive response of rocks. It reduces to the Biot theory if the stress and porosity responses are insensitive to the pore fluid's chemistry, i.e. if $S^k_{ij} = 0$ and $B^k = 0$. In this case the parameters L_{ijkl} and Q are seen to possess the meaning of the elastic stiffness matrix and the void compressibility, respectively.

A further simplification of the constitutive laws is obtained by incorporating in them information on the material's symmetry. To avoid mathematical complexities, we shall focus here exclusively on completely isotropic behaviour, even though shales are presumably more accurately described in terms of a transversely isotropic material, for which the constitutive relations are only invariant to rotations about one special axis. For isotropic materials, the tensors M_{ij} and S^k_{ij} are diagonal, i.e. they admit a representation in terms of the scalars ζ and ω of the form

$$M_{ij} = \zeta \delta_{ij}, \quad S^k_{ij} = \omega^k \delta_{ij} \tag{63}$$

and the elastic stiffness L_{ijkl} assumes the form of a fourth-order isotropic tensor, namely

$$L_{ijkl} = G(\delta_{ik}\delta_{jl} + \delta_{il}\delta_{jk}) + \left(K - \frac{2G}{3}\right)\delta_{ij}\delta_{kl} \tag{64}$$

The symbols G and K denote scalars that have the interpretation of the rock's shear and bulk modulus, respectively. With equations (62)–(64) we thus simplify equations (53) and (54) governing stress and pore fraction change to

$$\dot{\sigma}_{ij} = \left(K - \frac{2G}{3}\right)\dot{\varepsilon}_{kk}\delta_{ij} + 2G\dot{\varepsilon}_{ij} - \zeta\dot{p}\delta_{ij} + \sum_k \omega^k \dot{\mu}^k \delta_{ij} \tag{65}$$

and

$$\dot{v} = \zeta\dot{\varepsilon}_{ii} + Q\dot{p} + \sum_k B^k \dot{\mu}^k \tag{66}$$

We note that equation (65) can be written formally in the form of Hooke's law of linear elasticity if an effective stress σ^e_{ij} is defined so that

$$\sigma^e_{ij} = \sigma_{ij} + \left(\zeta p - \sum_k \omega^k \mu^k\right)\delta_{ij} \tag{67}$$

as then

$$\dot{\sigma}^e_{ij} = \left(K - \frac{2G}{3}\right)\dot{\varepsilon}_{kk}\delta_{ij} + 2G\dot{\varepsilon}_{ij} \tag{68}$$

Explicit relations between the various thermodynamic response coefficients entering equations (65) and (66) can be obtained on the assumption that not only the rock as a whole but also its solid constituent behaves in an elastic way, at least for low stresses. Denoting the bulk modulus of the solid matrix by K_s and using arguments discussed in detail in Appendix II, the void compressibility Q is then seen to be related to the scalar ζ according to

$$Q = (1/K_s)(\zeta - \phi) \tag{69}$$

while the equation

$$B^k = (1/K)(\zeta - 1)\omega^k \tag{70}$$

connects the parameters that characterize the response to fluid chemistry alterations. The quantity ζ turns out to be related to the bulk moduli K and K_s in a manner already familiar from poroelasticity, namely

$$\zeta = 1 - K/K_s \tag{71}$$

These expressions take a particularly simple form when the compressibility of the rock matrix is negligible in comparison to that of the bulk rock, i.e. when $K/K_s = 0$. In this situation, by equation (71), $\zeta = 1$ and also $Q = 0$ and $B^k = 0$, so that the constitutive equation (66) reduces to the simple statement

$$\dot{v} = \dot{\varepsilon}_{kk} \tag{72}$$

5.3. Electrolytic pore fluids

Although the discussion so far has been based on the assumption that the fluid is non-electrolytic, our results retain their validity for electrolytes as well. To see this, we follow the procedure used in Section 2 to obtain equation (10). Specifically, rather than summing over the

chemical potentials μ^k of the fluid components in equation (42), we sum over the electro-chemical potentials $\tilde{\mu}^\alpha$ of the ions present in the fluid. This replacement, however, leaves the form of the state equation (42) invariant, since

$$\sum_\alpha \tilde{\mu}^\alpha \dot{m}^\alpha = \sum_\alpha \mu^\alpha \dot{m}^\alpha = \sum_k \mu^k \dot{m}^k \tag{73}$$

on account of the requirement of local electroneutrality and chemical equilibrium (Reference 25, Section 1.19). As before, the index k runs over all components and the index α over all ionic species. Of course, the invariance property expressed by equation (73) could have been anticipated since the physical meaning of the free energy Ψ should be independent of whether we consider the chemical components or the ionic species as the 'substances' that make up the fluid. It follows from this observation that all conclusions that we have drawn from the state equation (42), such as the constitutive equations (65) and (66), hold true when the pore fluid is a solution of an electrolyte.

We again consider the case of a binary electrolyte in a little more detail. As discussed in the preceding section, the fluid consists of four ionic species in this case (water, undissociated electrolyte, cations, anions), even though there are only two chemical components present, namely the solvent, or diluent, and the solute. The chemical potential μ^S of the latter component is related through equation (20) to the chemical potential of the cations and anions comprising the electrolyte. For such a two-component system the constitutive relations (65) and (66) for the stress and volume fraction can be written as

$$\begin{aligned}\dot{\sigma}_{ij} = &\left(K - \frac{2G}{3}\right)\dot{\varepsilon}_{kk}\delta_{ij} + 2G\dot{\varepsilon}_{ij} - (\zeta - \omega^D/\bar{\rho}^D)\dot{p}\delta_{ij} \\ &+ (\omega^S - \omega^D\bar{\rho}^S/\bar{\rho}^D)(RT/M^S)(\ln a^S)^{\cdot}\delta_{ij}\end{aligned} \tag{74}$$

and

$$\dot{v} = \xi\dot{\varepsilon}_{ii} + (Q + B^D/\bar{\rho}^D)\dot{p} + (B^S - B^D\bar{\rho}^S/\bar{\rho}^D)(RT/M^S)(\ln a^S)^{\cdot} \tag{75}$$

where we used the Gibbs–Duhem equation (45) in the form

$$\dot{\mu}^D = (1/\bar{\rho}^D)(\dot{p} - \bar{\rho}^S\dot{\mu}^S) \tag{76}$$

to eliminate the chemical potential μ^D of the diluent (water) from the constitutive equations and observed that the solute chemical potential admits the representation

$$\mu^S = g^S(p, T) + \frac{RT}{M^S}\ln a^S \tag{77}$$

Here g^S denotes a standard function that depends at most on pressure and temperature, R is the gas constant, and M^S and a^S are the molar mass and the activity of the solute, respectively. Since the dependence of g^S on pressure is typically weak, we suppressed it in equations (74) and (75).

6. COMPLETE SET OF FIELD EQUATIONS

For future reference we list here the governing equations of our model for the constitutive behaviour of water-absorbing rocks. We focus on the situation of a pore fluid that is either a solution of a non-electrolyte or of a binary electrolyte. To avoid explicit consideration of the solution chemistry we assume the solution to be ideal, so that the solute activity a^S becomes equal to the solute mole fraction x^S, i.e.

$$a^S = x^S \tag{78}$$

Solutions approximate ideal behaviour when they are sufficiently dilute, i.e. when x^S is small. Note that the mole fraction x^S, which is, in general, related to the solute mass fraction c^S through

$$c^S = x^S M^S / (x^S M^S + (1 - x^S) M^D) \tag{79}$$

where M^D is the molar mass of the diluent, becomes directly proportional to x^S in dilute solutions, as then

$$c^S = \frac{M^S}{M^D} x^S \tag{80}$$

The constitutive equations (74) and (75) specify the alteration in solid stress and volume fraction in terms of five independent variables, namely the three displacements u_i ($i = 1, 2, 3$), from which the solid strains ε_{ij} are derivable (according to $\varepsilon_{ij} = \partial u_i / \partial x_j$), the pore pressure p and the solute mole fraction x^S. These fields must obey the mechanical equilibrium condition

$$\frac{\partial \sigma_{ij}}{\partial x_j} = 0 \tag{81}$$

and they must respect the conservation equations of fluid and solute mass, which provide for an incompressible fluid the statements

$$\dot{v} + \operatorname{div} \mathbf{u} = 0 \tag{82}$$

and

$$\bar{\rho}_f v \dot{c}^S + \bar{\rho}_f \mathbf{u} \cdot \operatorname{grad} c^S + \operatorname{div} \mathbf{J}^S = 0 \tag{83}$$

as shown in Appendix III. Specifically, these fields must obey the equations

$$(K - 2G/3) \frac{\partial^2 \dot{u}_k}{\partial x_k \partial x_i} + 2G \frac{\partial^2 \dot{u}_i}{\partial x_j \partial x_j} + \omega^D \dot{p} \frac{\partial (1/\bar{\rho}^D)}{\partial x_i} - (\zeta - \omega^D / \bar{\rho}^D) \frac{\partial \dot{p}}{\partial x_i}$$
$$- \omega^D (RT/M^S) (\ln c^S)^{\cdot} \frac{\partial (\bar{\rho}^S / \bar{\rho}^D)}{\partial x_i} + (\omega^S - \omega^D \bar{\rho}^S / \bar{\rho}^D)(RT/M^S) \frac{\partial (\ln c^S)^{\cdot}}{\partial x_i} = 0 \tag{84}$$

$$\zeta \frac{\partial \dot{u}_i}{\partial x_i} + (Q + B^D / \bar{\rho}^D) \dot{p} + (B^S - B^D \bar{\rho}^S / \bar{\rho}^D)(RT/M^S) (\ln c^S)^{\cdot}$$
$$- \frac{k}{\nu} \frac{\partial^2 p}{\partial x_i^2} - \bar{\rho}_f r \frac{RT}{M^S} \frac{\partial}{\partial x_i} \left(\frac{1}{c^S c^D} \frac{\partial c^S}{\partial x_i} \right) = 0 \tag{85}$$

and

$$\bar{\rho}_f v \dot{c}^S - \left(\bar{\rho}_f \frac{k}{\nu} \right) \left(\frac{\partial p}{\partial x_i} - r \frac{\bar{\rho}_f}{c^D} \frac{\partial \mu^S}{\partial c^S} \frac{\partial c^S}{\partial x_i} \right) \frac{\partial c^S}{\partial x_i} - L \bar{\rho}_f \frac{\partial}{\partial x_i} \left(\frac{1}{p} \frac{\partial p}{\partial x_i} \right) - \bar{\rho}_f D \frac{\partial^2 c^S}{\partial x_i^2} = 0 \tag{86}$$

Equation (84) is obtained by introducing the constitutive equation (74) for the stress rate into the equilibrium (81); equation (85) follows from (82) if one uses the constitutive equation (75) and the transport equation (25) to eliminate, respectively, $\dot{v}$ and $\mathbf{u}$; equation (86) results from substituting the transport equations (25) and (26) into the conservation equation (83) for the solute mass. In arriving at equations (85) and (86) we invoked equation (80), which in conjunction with equation (78) allows us to replace $(\ln a^S)^{\cdot}$ by $(\ln c^S)^{\cdot}$.

7. NUMERICAL SOLUTIONS

The coupled and complex character of the set of differential equations (84)–(86) prevents us from obtaining analytical solutions. We thus take recourse to a finite-element numerical scheme (the workings of which are described in Appendix IV), to obtain insight into the constitutive response predicted by our model. Using it, we simulate a laboratory experiment designed for studying the interaction of fluid with a shale, a specific water-absorbing rock, and then analyse the evolution of stress and strain around a wellbore in shale through which drilling fluid has been lost to the formation.

7.1. Simulation of an experiment

The experimental set-up is depicted in Figure 1.[32,33] A cylindrical shale sample is exposed at its opposing faces (Chambers A and B) to distilled water of equal pressure while being subjected to uniaxial stress acting along the axis of the sample. The external load is applied through porous plates. The chemistry of the fluid in Chamber A is then altered by adding salt to it while maintaining the fluid pressure. We are interested here in the pressure evolution in Chamber B and the swelling of the shale sample when it is exposed to fluids of different chemistry.

The fluid pressure response in Chamber B predicted by our theory is shown in Figure 2. The simulation assumes both swelling parameters ω^S and ω^D to be zero, but qualitatively similar results were obtained for non-zero values of these parameters. The matrix compressibility was

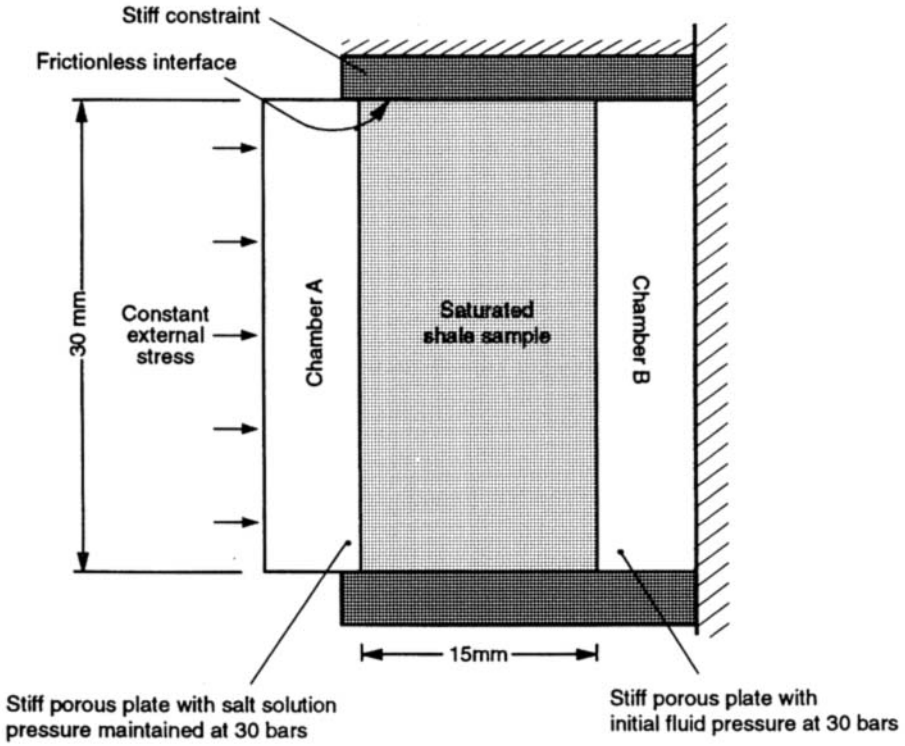

Figure 1. Schematic view of experimental set-up

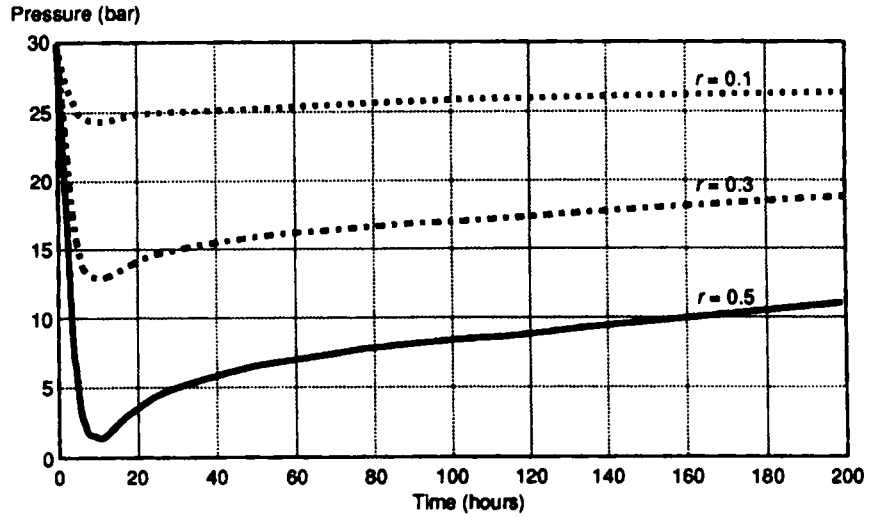

Figure 2. Predicted pressure changes in Chamber B in response to addition of salt in Chamber A ($k/v = 5 \times 10^{-6}$ mm^3/kg/s, $D = 1 \times 10^{-4}$ mm^2/s). The changes are depicted for three values of the reflection coefficient r

regarded as negligible, i.e. $K/K_s = 0$ (so that, by equations (120) and (121) $\bar{\omega} = 0$ and $q = 0$). The Young's modulus E, Poisson's ratio, diffusion coefficient D, and the permeability/viscosity ratio k/v were taken to be 2 GPa, 0·3, 1×10^{-4} mm^2/s and 5×10^{-6} mm^3/kg/s. Pressure diffusion effects were neglected, i.e. $L = 0$. The figure indicates that the fluid pressure in Chamber B decreases rapidly even though the pressure in Chamber A remained constant. After a while, the fluid pressure in Chamber B increases slowly and approaches its original value. The initial pressure-drop was more pronounced when the reflection coefficient r was high; longer times were therefore required to restore the pressure in Chamber B to its initial value.

The pressure behaviour we observed in our simulations is indeed seen in experiments;[33] it is indicative of shale acting as an (imperfect) osmotic barrier to solute (salt) transport. The mobility difference between solute and solvent in the shale causes an osmotic pressure differential between the chambers to develop when the fluid salinity in Chamber A is changed. This osmotic pressure differential vanishes in the course of time, however, as diffusion equalizes the salt concentration in the chambers (Figure 3).

Figure 4 shows the swelling of the shale sample with time as predicted by our theory. In these simulations we used educated guesses to fill in the gaps in the input data for some of the parameters in the model. Specifically, we took ω^S and ω^D to be equal to the same value of $100\, M^S/RT$. Unfortunately, we were not able to find any experimental result that we could compare with our simulation results with respect to chemically induced shale deformation. Nevertheless, the predictions of our model tie in nicely with other experimental evidence on the swelling behaviour of rocks. Thus, Kranz *et al.*[8] measured the confined radial and axial expansion of tuff rocks immersed in water as a function of time. They found shapes of the swelling curves that are very similar to the ones in Figure 4 in that the swelling rate continuously decreases with time to approach a constant swelling strain.

Experiments on the effect of fluid chemistry on the swelling of shale have been performed by Steiger,[34] who measured the swelling pressure, i.e. the pressure needed to suppress volumetric swelling for various concentrations of the binary electrolytes KCl and NaCl. The experiments showed that the swelling pressure, and therefore also the swelling strain, decreases with increasing

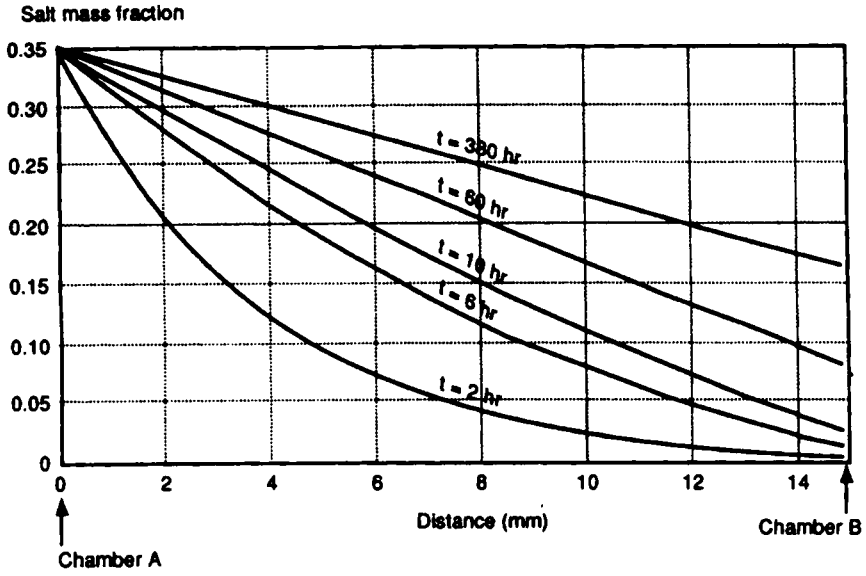

Figure 3. Transient salt concentration distribution in shale sample

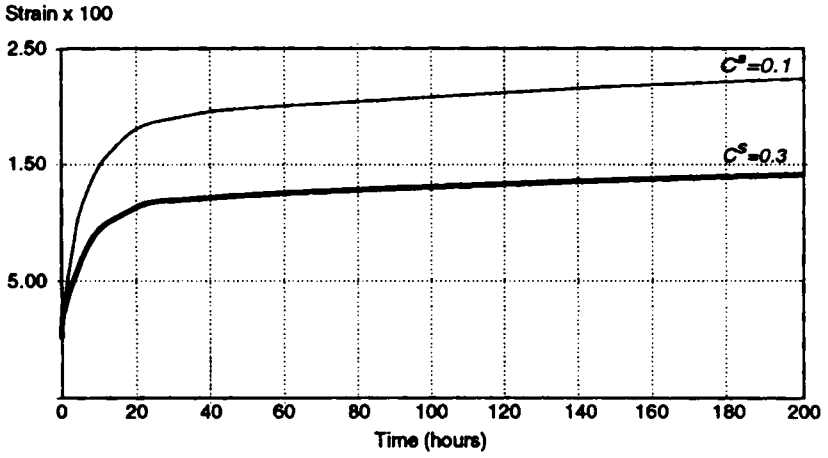

Figure 4. Numerical simulation of the swelling of the shale sample for two salt concentrations c^s in Chamber A (Young's modulus = 2 GPa, Poisson's ratio = 0·3, reflection coefficient = 0·3)

salt concentration. This is in qualitative agreement with the simulation results depicted in Figure 4 and lends further credibility to the constitutive model proposed here.

7.2. Hydration stresses and strains around a wellbore

We finally use our model to simulate the changes in stress and strain that occur in a shale formation when it is invaded by drilling fluid from a wellbore. Understanding these changes can help one to decide on operational measures that mitigate the costly effects of wellbore instabilities in these formations.

Adapting our finite-element solution procedure to accommodate the radial wellbore geometry is straightforward and deserves no further comment. With this modification in place, we consider an infinite formation that is subject to a horizontally compressive far-field isotropic stress (taken as 10 MPa). Drilling fluid (pressure 5 MPa; initial salt mass fraction $c^S = 0{\cdot}1$) is allowed to invade the formation (initial formation fluid pressure 0 MPa) from a vertical wellbore (radius 10 cm). The physical characteristics of the shale and the fluid are as in the previous example. Figure 5

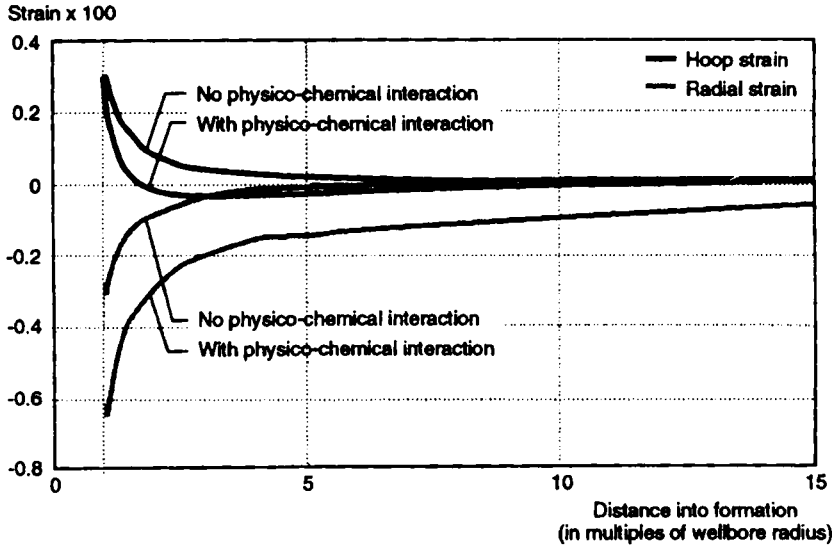

Figure 5. Deformation of the near-wellbore formation resulting from drilling fluid invasion (reflection coefficient = 0, salt mass fraction = 0·1)

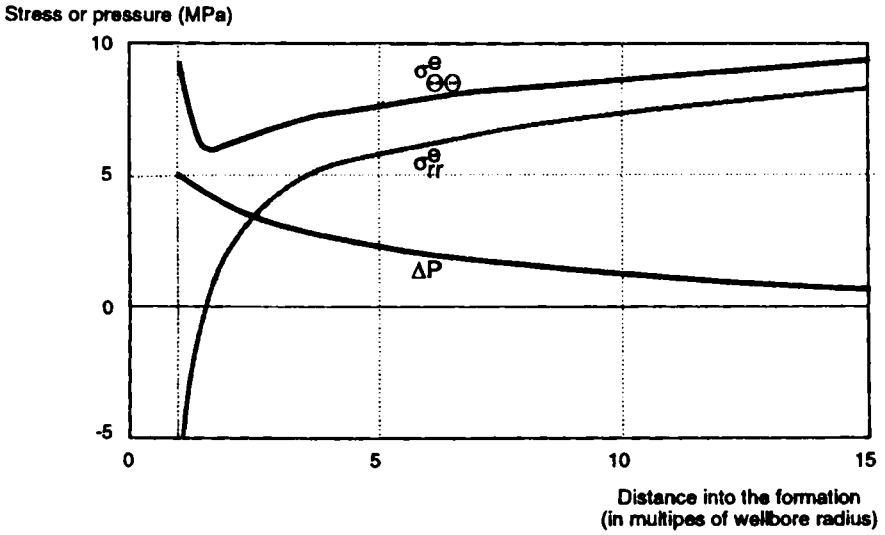

Figure 6. Stress distribution around the wellbore when a physico-chemical interaction between drilling fluid and formation is operative

depicts the variation in radial and hoop (tangential) strain around the wellbore when a steady state is reached, with ($\omega^S = \omega^D = 100M^S/RT$) and without ($\omega^S = \omega^D = 0$) drilling fluid/shale interaction. In both situations the radial strain is negative, i.e. directed towards the wellbore, to accommodate the removal of the far-field stresses from the circumference of the wellbore that is associated with the drilling process. However, as seen in the figure, physico-chemical interaction

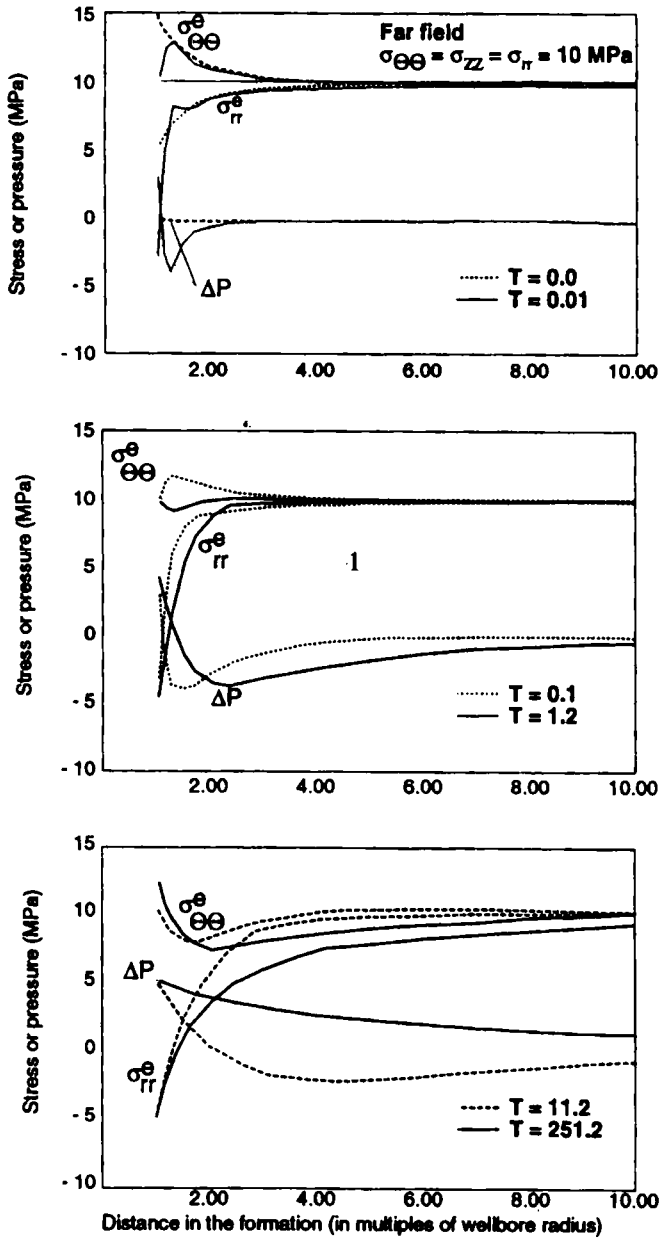

Figure 7. Evolution of effective radial stres, effective hoop stress and pore pressure as a function of dimensionless time T

effects enhance the deformation experienced by the wellbore wall, with obviously detrimental consequences for borehole stability.

A different view of the same situation is shown in Figure 6, in which we plot the near-wellbore variations in effective radial (σ'_{rr}) and hoop ($\sigma'_{\theta\theta}$) stress (see equation (67) for the effective stress concept in swelling rocks), together with the difference Δp between current and initial formation fluid pressure when fluid/shale interaction processes are operative and a steady state has been reached. Even though the wellbore wall is stabilized by a drilling fluid pressure of 5 MPa, the effective radial stress experienced by the well-bore wall is negative. i.e. tensile, thereby promoting tensile failure of the near-wellbore formation.

Figure 7 provides information about the evolution of the radial and tangential effective stresses, and of the formation pressure change. The figure depicts the spatial distribution of these quantities for various values of dimensionless time $T = Dt/d^2$, where D is the diffusion coefficient, taken as 1×10^{-4} mm^2/s, and d denotes the borehole radius (10 cm). It is seen that tensile radial stresses develop first at the wellbore walls and that ongoing fluid invasion increases the size of the region in the formation that experiences this stress condition. As indicated in the figure, the formation pressure in front of the invasion zone decreases below its initial value, i.e. Δp is negative in this region. The effect is related to the increase in pore volume the formation experiences as it expands to accommodate the invasion fluid.

The difference between radial stress and hoop stress, $\sigma_{rr} - \sigma_{\theta\theta}$, provides a measure for the shear stress experienced by the formation. The development of this quantity can be read off from Figure 7, but it is shown for clarity as a collection of plots in Figure 8. In the immediate vicinity of the wellbore the shear stress increases monotonically with time; its variation outside this region is more complex. In any case, when steady state is reached, each location in the formation is subject to a higher shear stress than it would be without drilling-fluid invasion. The relevance of this observation lies in the fact that, according to the Mohr–Coulomb criterion, a high value of $\sigma_{rr} - \sigma_{\theta\theta}$ promotes shear failure.

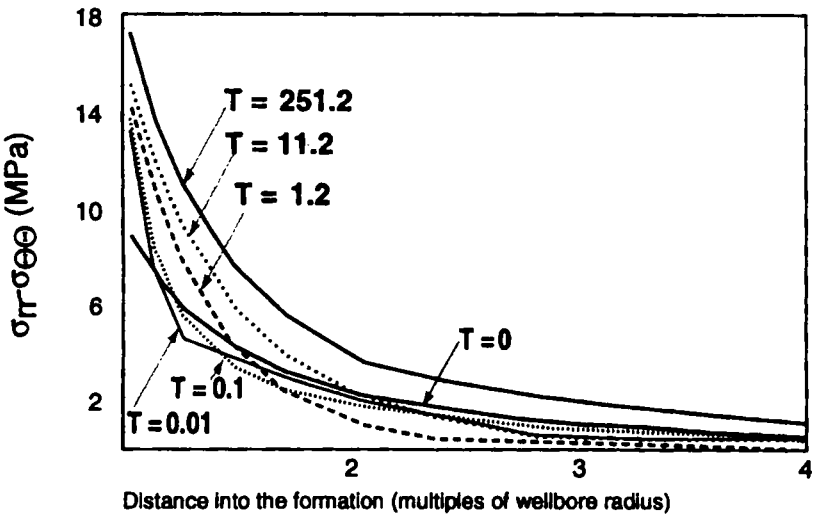

Figure 8. Evolution of shear stress as a function of dimensionless time

8. DISCUSSION AND FUTURE WORK

The development of our model of hydration swelling has been guided by theoretical principles and by our desire, expressed through a series of assumptions, to keep the model as simple as possible. Although this emphasis on theoretical considerations is certainly justified, and indeed necessary, to get the fundaments of the constitutive model in place, it is clear that any further refinement of our model requires dedicated experimental work. Experiments are necessary not only to obtain data for some of the parameters entering our theory but also to check the validity of the assumptions introduced. We have in mind here, in particular, the assumptions concerning elastic deformation of the mineral matrix and the persistence of local physico-chemical equilibrium. The elasticity assumption is certainly not generally warranted for the rock types that have been the subject of this investigation, yet going beyond it cannot be achieved by theoretical reasoning alone. Such an advancement would have to wait until a concerted effort of both theory and experiment provides a failure criterion for the model that accounts for the effect of the pore fluid chemistry.[34–36]

Replacing the local chemical equilibrium assumption used in this study by a non-equilibrium reaction rate model does not amount to entering theoretically unchartered waters; it only means venturing beyond the familiar harbour of textbook continuum thermodynamics. However, such a step towards generalizing the present model appears justified only if deemed necessary by experimental evidence, if good experimental characterization of the hydration reaction is available, and if one is prepared to accept the additional degree of complexity in the constitutive model that follows such a line of investigation.

APPENDIX I

Derivation of the balance equation for the Helmholtz free energy

The fundamental balance equation for thermodynamically open systems can be formulated in a generic way as

$$\left(\int_R \pi \, dv\right)^{\cdot} = \int_{\partial R} \mathbf{j}_{\pi,\mathrm{ncon}} \cdot \mathbf{n} \, da + \int_{\partial R} \mathbf{j}_{\pi,\mathrm{con}} \cdot \mathbf{n} \, da + \int_R r_\pi \, dv \tag{87}$$

in which the symbol π denotes the bulk density of some (extensive) thermodynamic quantity defined in region R. The term $\mathbf{j}_{\pi,\mathrm{con}}$, which specifies the convective flux of π into R (i.e. the influx of π associated with fluid flow), extends the usual, closed-system form of the balance equation[37] to open systems. The quantity $\mathbf{j}_{\pi,\mathrm{ncon}}$ denotes the non-convective flux of π, r_π is a source term pertaining to the production of π within R, and $\mathbf{n}$ is the outward unit normal vector on ∂R. The time derivative indicated by the dot accent on the left-hand side of equation (87) is the derivative that 'follows' the motion of the solid, i.e.

$$\dot{\pi} = \frac{\partial \pi}{\partial t} + \mathbf{v}_s \cdot \operatorname{grad} \pi \tag{88}$$

where $\mathbf{v}_s$ denotes the local solid velocity.

A pair of balance equations, one for the internal energy and the other for the entropy, are thus obtained merely by identifying the generic quantity π in equation (87) first with the density of internal energy ε and then with the density of entropy η. The corresponding non-convective fluxes

$\mathbf{j}_{\pi,\mathrm{ncon}}$ assume their familiar forms from continuum mechanics.[37] Specifically, the non-convective flux of internal energy is represented by

$$\mathbf{j}_{\varepsilon,\mathrm{ncon}} = \boldsymbol{\sigma}\mathbf{v}_s - \mathbf{q} \tag{89}$$

and that of entropy by

$$\mathbf{j}_{\eta,\mathrm{ncon}} = -\mathbf{q}/T \tag{90}$$

In these equations the symbols $\mathbf{q}$, T and $\boldsymbol{\sigma}$, respectively, denote heat flux, temperature and the Cauchy stress tensor. The convective internal energy and entropy fluxes we specify according to

$$\mathbf{j}_{\varepsilon,\mathrm{con}} = -\sum_k h^k \mathbf{I}^k \tag{91}$$

and

$$\mathbf{j}_{\eta,\mathrm{ncon}} = -\sum_k \eta^k \mathbf{I}^k \tag{92}$$

where the sum in both expressions extends over all fluid components. Here, $\mathbf{I}^k$ denotes the mass flux of the kth fluid component with respect to the solid phase, i.e.

$$\mathbf{I}^k = \rho^k(\mathbf{v}^k - \mathbf{v}_s) \tag{93}$$

The terms $\mathbf{v}^k$, ρ^k, h^k and η^k denote, respectively, the velocity, mass density, specific enthalpy and specific entropy of this fluid component. Expressions (91) and (92) for the convective fluxes of internal energy and entropy are the same as those used in engineering thermodynamics to describe the exchange of energy and entropy in open thermodynamic systems. Extensive discussions about the structure of these terms can be found in the pertinent textbook literature (e.g. References 38 and 39; also Reference 25, Section 4.6).

Recalling from elementary continuum mechanics that the production of internal energy vanishes, i.e. $r_\varepsilon = 0$, when body force fields are absent, as is assumed here, and denoting by γ the entropy production, i.e. $\gamma \equiv r_\eta$, we use the above expressions to write the balances of internal energy and entropy for region R as

$$\left(\int_R \varepsilon \mathrm{d}v\right)^{\cdot} = \int_{\partial R} (\boldsymbol{\sigma}\mathbf{v}_s - \mathbf{q})\cdot\mathbf{n}\,\mathrm{d}a - \int_{\partial R}\sum_k h^k \mathbf{I}^k \cdot \mathbf{n}\,\mathrm{d}a \tag{94}$$

and

$$\left(\int_R \eta\,\mathrm{d}v\right)^{\cdot} = -\int_{\partial R}\frac{\mathbf{q}}{T}\cdot\mathbf{n}\,\mathrm{d}a - \int_{\partial R}\sum_k \eta^k \mathbf{I}^k\cdot\mathbf{n}\,\mathrm{d}a + \int_R \gamma\,\mathrm{d}v \tag{95}$$

By combining these two equations, recalling that the Helmholtz free energy density ψ is related to densities of internal energy and entropy through $\psi = \varepsilon - T\eta$, and using the thermodynamic identity $\mu^k = h - T\eta^k$ (e.g. Reference 25, Section 1.10) for the chemical potentials μ^k, we immediately obtain equation (1).

APPENDIX II

Relations between the response parameters

The parameters ζ, Q, ω^k and B^k introduced in the constitutive relations (65) and (66) can be further characterized if we make additional but plausible assumptions on the way water-absorbing rock behaves in response to mechanical and chemical loading.

We consider the case of a rock sample that is infiltrated by and in free hydraulic communication with ambient pore fluid of fixed and homogeneous composition. If we now assume that the rock *matrix* behaves linear elastically, then it can be shown that the parameter ζ is related to K_s, the bulk modulus of the solid matrix, according to equation (71) and furthermore that equation (69) for Q holds.[40,41] The argument starts from the observation that the loading increment

$$\dot{\sigma}_{ij} = -\dot{p}\delta_{ij} \tag{96}$$

produces the local stress alteration $-\dot{p}\delta_{ij}$ at each point both in the elastic solid and the fluid. Associated with it is the strain rate

$$\dot{\varepsilon}_{ij} = -\frac{\dot{p}}{3K_s}\delta_{ij} \tag{97}$$

and the volume change

$$\dot{v} = -\phi\frac{\dot{p}}{K_s} \tag{98}$$

Equation (71) then results after one uses equations (96) and (97) in the constitutive relation (65) for the stresses, and equation (69) follows from employing relations (96) and (98) in the constitutive relation (66) for the volume change. In both cases one should note that the chemical composition of the fluid remains unchanged and hence its chemical potentials do not vary.

Next, we focus on the behaviour of the shale sample in response to alterations of pore fluid chemistry. It appears naturally to assume that, at least to a first approximation, the volumetric strain rate produced through alteration of the fluid composition (swelling) at conditions of constant pore pressure and stress is accompanied by an equal change in the pore volume fraction, i.e. that

$$\dot{\varepsilon}_{ii} = \dot{v} \tag{99}$$

when $\dot{p} = 0$ and $\dot{\sigma}_{ij} = 0$. From the constitutive relation (65) we find that

$$\dot{\varepsilon}_{ii} = -\frac{1}{K}\sum_k \omega^k \dot{\mu}^k \tag{100}$$

when there is no mechanical loading, while the relation (66) for $\dot{v}$ yields

$$\dot{v} = -\frac{\zeta}{K}\sum_k \omega^k \dot{\mu}^k + \sum_k B^k \dot{\mu}^k \tag{101}$$

after ε_{ii} is eliminated using equation (100). From the last two expressions it is seen that relation (70) must indeed hold to ensure the validity of requirement (99).

APPENDIX III

Alternative forms of the conservation equations for the fluid's component masses

We start from equation (7) for the fluid's partial masses. Eliminating the fluxes $\mathbf{I}^k$ in favour of the diffusion fluxes $\mathbf{J}^k$ using the mathematical identity (13) and observing the relation (8) between mass density ρ^k and intrinsic mass density $\bar{\rho}^k$, one finds

$$(\phi\bar{\rho}^k)^{\cdot} - \mathbf{v}_s \cdot \operatorname{grad}(\phi\bar{\rho}^k) + \operatorname{div}(\phi\bar{\rho}^k\mathbf{v}_f) + \operatorname{div}\mathbf{J}^k = 0 \tag{102}$$

Multiplying both sides of that equation by the volume ratio J (40) and using the Euler identity (41), one can transform it into

$$(v\bar{\rho}^k)^{\cdot} + J\,\mathrm{div}(\bar{\rho}^k\mathbf{u}) + J\,\mathrm{div}\,\mathbf{J}^k = 0 \tag{103}$$

where v and $\mathbf{u}$, respectively, denote the pore volume fraction and the filter velocity, these quantities being defined by equations (47) and (15). Next, we select as reference the configuration at any given instant. For this choice J is unity although that does not mean that the time derivative of J vanishes. Assuming further that the fluid is incompressible, we obtain

$$\bar{\rho}_f(\dot{v}c^k + v\dot{c}^k) + \bar{\rho}_f\,\mathrm{div}(c^k\mathbf{u}) + \mathrm{div}\,\mathbf{J}^k = 0 \tag{104}$$

where we introduced the mass fraction $c^k = \bar{\rho}^k/\bar{\rho}_f$. As $\sum_k c^k = 1$ and $\sum_k \mathbf{J}^k = 0$, summing over all fluid components yields the equation

$$\dot{v} + \mathrm{div}\,\mathbf{u} = 0 \tag{105}$$

which provides the statement of the mass conservation for the fluid as a whole that we used in Section 6. Invoking equation (105) allows us to transform equation (104) to the form

$$\bar{\rho}_f v\dot{c}^k + \bar{\rho}_f\mathbf{u}\cdot\mathrm{grad}\,c^k + \mathrm{div}\,\mathbf{J}^k = 0 \tag{106}$$

which was used in the main body of the text.

APPENDIX IV

Numerical implementation

In preparation for their numerical solution we rewrite equatons (84)–(86) in matrix form. To this end, we regard the stress and strain tensors $\boldsymbol{\sigma}$ and $\boldsymbol{\varepsilon}$ as vectors in a six-dimensional space in which they have representations

$$\boldsymbol{\sigma} = [\sigma_{11}, \sigma_{22}, \sigma_{33}, \sigma_{12}, \sigma_{23}, \sigma_{31}]^{\mathrm{T}} \tag{107}$$

and

$$\boldsymbol{\varepsilon} = [\varepsilon_{11}, \varepsilon_{22}, \varepsilon_{33}, 2\varepsilon_{12}, 2\varepsilon_{23}, 2\varepsilon_{31}]^{\mathrm{T}} \tag{108}$$

Upon further introducing the vector

$$\mathbf{m} = [1, 1, 1, 0, 0, 0]^{\mathrm{T}} \tag{109}$$

and the symmetric 6×6 matrix

$$\mathbf{D} = \begin{pmatrix} K+(4/3)G & K-(2/3)G & K-(2/3)G & 0 & 0 & 0 \\ K-(2/3)G & K+(4/3)G & K-(2/3)G & 0 & 0 & 0 \\ K-(2/3)G & K-(2/3)G & K+(4/3)G & 0 & 0 & 0 \\ 0 & 0 & 0 & G & 0 & 0 \\ 0 & 0 & 0 & 0 & G & 0 \\ 0 & 0 & 0 & 0 & 0 & G \end{pmatrix} \tag{110}$$

the constitutive equation for the stress (74) takes the form

$$\dot{\boldsymbol{\sigma}} = \mathbf{D}\dot{\boldsymbol{\varepsilon}} - \alpha\mathbf{m}\dot{p} + \omega\mathbf{m}\dot{c}^{\mathrm{S}} \tag{111}$$

in which we invoked the abbreviations

$$\alpha = \zeta - \omega^{D}/\bar{\rho}^{D} \tag{112}$$

and

$$\omega = (\omega^{S} - \omega^{D}(\bar{\rho}^{S}/\bar{\rho}^{D}))\,(RT/M^{S})\,(1/c^{S}) \tag{113}$$

We also introduce the matrix differential operator

$$\mathbf{L} = \begin{pmatrix} \partial/\partial x_1 & 0 & 0 & \partial/\partial x_2 & 0 & \partial/\partial x_3 \\ 0 & \partial/\partial x_2 & 0 & \partial/\partial x_1 & \partial/\partial x_3 & 0 \\ 0 & 0 & \partial/\partial x_3 & 0 & \partial/\partial x_2 & \partial/\partial x_1 \end{pmatrix}^{T} \tag{114}$$

so that we can express the kinematic relation between the displacement vector $\mathbf{r} = [u_1, u_2, u_3]$ and strain $\boldsymbol{\varepsilon}$ as

$$\boldsymbol{\varepsilon} = \mathbf{L}\mathbf{r} \tag{115}$$

and rewrite the mechanical equilibrium requirement (81) as

$$\mathbf{L}^{T}\dot{\boldsymbol{\sigma}} = \mathbf{0} \tag{116}$$

Combining (111), (115) and (116), we obtain

$$\mathbf{L}^{T}(\mathbf{D}\mathbf{L}\dot{\mathbf{r}} - \alpha\mathbf{m}\dot{p} + \omega\mathbf{m}\dot{c}^{S}) = \mathbf{0} \tag{117}$$

which is merely equation (84) in matrix form.

Expressing equations (85) and (86) in terms of matrices is straightforward. One finds

$$\zeta\mathbf{m}^{T}\mathbf{L}\dot{\mathbf{r}} + q\dot{p} + \bar{\omega}\dot{c}^{S} - k/\nu\nabla^{T}\nabla p - rL_{D}\nabla^{T}\nabla c^{S} = 0 \tag{118}$$

and

$$\phi\dot{c}^{S} - L_{p}\nabla^{T}\nabla p - D\nabla^{T}\nabla c^{S} = 0 \tag{119}$$

where

$$q = Q + B^{D}/\bar{\rho}^{D} \tag{120}$$

$$\bar{\omega} = (B^{S} - B^{D}(\bar{\rho}^{S}/\bar{\rho}^{D}))\,(RT/M^{S})\,(1/c^{S}) \tag{121}$$

$$L_{D} = \bar{\rho}_{f}(RT/M^{S})\,(1/c^{S}c^{D})) \tag{122}$$

and

$$L_{p} = L/p \tag{123}$$

In equation (119) we neglected a convection term $\mathbf{u}\cdot\operatorname{grad} c^{S}$. Thus assumption, which simplifies the numerical solution procedure considerably, is warranted in rock of very low permeability.

To solve the matrix equations (117)–(119), we use a Galerkin finite-element method to find the spatial dependence of the variables $\mathbf{r}$, p, c^{S} and a one-step finite-difference procedure to integrate over time. Extensive discussions of these standard methods can be found in the literature,[42–44] so our discussion can be brief.

We partition the region Ω, for which we seek to determine the fields, into finite elements. Within each element we approximate the variations in $\mathbf{r}$, p and c^{S} in terms of the values $\mathbf{r}_i$, p_i and c_i^{S} these fields assume at a number of finite points within or on the boundary of an element. Accordingly, we write

$$\mathbf{r} = \sum_{i=1}^{n} N_{r_i}\mathbf{r}_i, \quad p = \sum_{i=1}^{n} N_{p_i}p_i, \quad c^{S} = \sum_{i=1}^{n} N_{c_i}c_i^{S} \tag{124}$$

where n denotes the number of nodes, and N_{r_i}, N_{p_i} and N_{c_i} are interpolating or shape functions of polynomial character.

In the Galerkin method the shape functions are also used to construct the weak form of the equations under consideration. Proceeding in the standard way, one finds in our case that

$$\mathbf{K}\dot{\mathbf{r}} - \mathbf{A}\dot{\mathbf{p}} + \mathbf{W}\dot{\mathbf{c}}^S = \dot{\mathbf{f}} \tag{125}$$

$$\mathbf{A}^T\dot{\mathbf{r}} + \mathbf{S}\dot{\mathbf{p}} + \hat{\mathbf{M}}\dot{\mathbf{c}}^S + \mathbf{H}_H\mathbf{p} + \mathbf{D}_H\mathbf{c}^S = \mathbf{0} \tag{126}$$

$$\mathbf{M}\dot{\mathbf{c}}^S + \mathbf{H}_D\mathbf{p} + \mathbf{D}_D\mathbf{c}^S = \mathbf{0} \tag{127}$$

where

$$\mathbf{K} = -\int_\Omega (\mathbf{L}\mathbf{N}_r)^T\mathbf{D}(\mathbf{L}\mathbf{N}_r)\,d\Omega, \quad \mathbf{A} = \int_\Omega (\mathbf{L}\mathbf{N}_r)^T\alpha\mathbf{m}\mathbf{N}_p\,d\Omega$$

$$\mathbf{W} = \int_\Omega (\mathbf{L}\mathbf{N}_r)^T\omega\mathbf{m}\mathbf{N}_c\,d\Omega, \quad \mathbf{S} = \int_\Omega \mathbf{N}_p^T q\mathbf{N}_p\,d\Omega$$

$$\hat{\mathbf{M}} = \int_\Omega \mathbf{N}_p^T\bar{\omega}\mathbf{N}_c\,d\Omega, \quad \mathbf{H}_H = \int_\Omega (\nabla\mathbf{N}_p)^T(k/\nu)(\nabla\mathbf{N}_p)\,d\Omega \tag{128}$$

$$\mathbf{D}_H = \int_\Omega (\nabla\mathbf{N}_p)^T\mathbf{r}L_D(\nabla\mathbf{N}_c)\,d\Omega, \quad \mathbf{M} = \int_\Omega \mathbf{N}_c^T\phi\mathbf{N}_c\,d\Omega$$

$$\mathbf{H}_D = \int_\Omega (\nabla\mathbf{N}_c)^T L_p(\nabla\mathbf{N}_p)\,d\Omega, \quad \mathbf{D}_D = \int_\Omega (\nabla\mathbf{N}_c)^T D(\nabla\mathbf{N}_c)\,d\Omega$$

$$\mathbf{f} = -\int_\Gamma \mathbf{N}_r^T\hat{\mathbf{t}}\,d\Gamma$$

The symbols $\mathbf{N}_r$, $\mathbf{N}_p$ and $\mathbf{N}_c$ denote the vectors in the n-dimensional space that are formed from the shape functions N_{r_i}, N_{p_i}, N_{c_i}, and $\hat{\mathbf{t}}$ is the traction on the surface Γ that bounds Ω. The form of the finite-element matrices $\mathbf{A}$, $\mathbf{H}_H$, $\mathbf{D}_H$, $\mathbf{D}_{\dot{H}}$, $\mathbf{H}_D$, $\mathbf{D}_D$ incorporates the boundary conditions of the problem (see Figure 9).

The set of equations (125), (126) and (127) can be arranged into a first-order differential equation of the form

$$\mathbf{a}\dot{\mathbf{x}} + \mathbf{b}\mathbf{x} = \dot{\mathbf{q}} \tag{129}$$

where

$$\mathbf{a} = \begin{pmatrix} \mathbf{K} & -\mathbf{A} & \mathbf{W} \\ \mathbf{A}^T & \mathbf{S} & \hat{\mathbf{M}} \\ \mathbf{0} & \mathbf{0} & \mathbf{M} \end{pmatrix}, \quad \mathbf{b} = \begin{pmatrix} \mathbf{0} & \mathbf{0} & \mathbf{0} \\ \mathbf{0} & \mathbf{H}_H & \mathbf{D}_H \\ \mathbf{0} & \mathbf{H}_D & \mathbf{D}_D \end{pmatrix} \tag{130}$$

$$\mathbf{q} = \begin{pmatrix} \mathbf{f} \\ \mathbf{0} \\ \mathbf{0} \end{pmatrix}, \quad \mathbf{x} = \begin{pmatrix} \mathbf{r} \\ \mathbf{p} \\ \mathbf{c}^S \end{pmatrix} \tag{131}$$

To solve equation (129), we use a one-step finite-difference scheme whereby the solution $\mathbf{x}$ in the time interval from t to $t + \Delta t$ is assumed to vary linearly between its respective starting and ending values $\mathbf{x}_t$ and $\mathbf{x}_{t+\Delta t}$ according to

$$\mathbf{x} = \Theta\mathbf{x}_t + (1 - \Theta)\mathbf{x}_{t+\Delta t} \tag{132}$$

the symbol Θ, $0 < \Theta < 1$, denoting a time weighting factor. Depending on the selection of Θ various familiar time-stepping schemes are obtained.

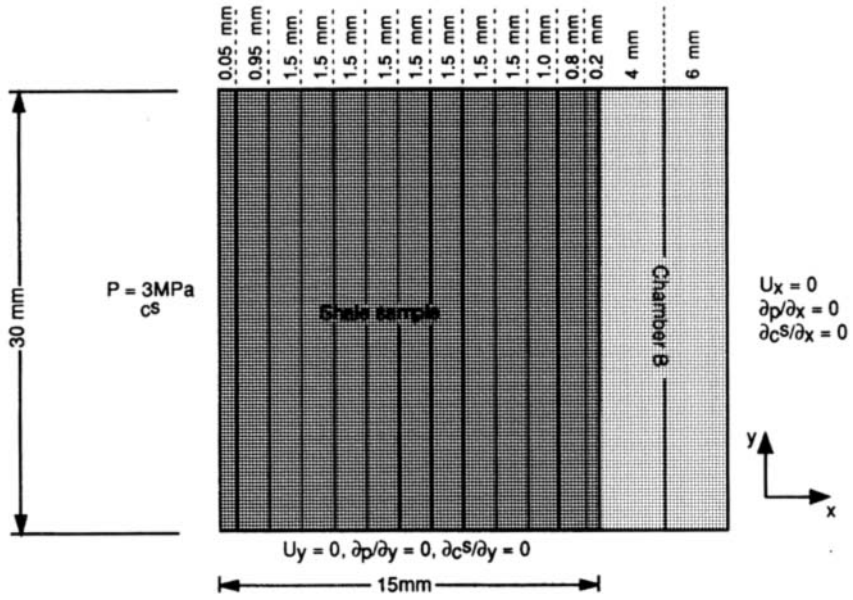

Figure 9. Boundary conditions and finite-element mesh for the numerical simulation (not to scale)

The boundary conditions that we used in the simulation are shown in Figure 9. The shale sample is discretized in the direction of the x-coordinate axis into 15 elements, and Chamber B is represented by two elements. Two-dimensional, eight-node, quadrilateral-element interpolation functions are used to approximate the displacement field and two-dimensional, four-node, quadrilateral-element interpolation functions for the pore pressure and concentration approximation. This choice of an 8–4 node combination enhances numerical stability.[45,46]

REFERENCES

1. H. van Olphen, *An Introduction to Clay Colloid Chemistry*, 2nd edn, Wiley, New York, 1977.
2. J. K. Mitchell, *Fundamentals of Soil Behaviour*, 2nd edn, Wiley, New York, 1993.
3. J. N. Israelachvili, *Intermolecular and Surface Forces*, 2nd edn, Academic Press, London, 1991.
4. B. E. Viani, P. F. Low and C. B. Roth, 'Direct measurement of the relation between interlayer force and interlayer distance in the swelling of montmorillonite', *J. Colloid Interface Sci.*, **96**, 229–244 (1983).
5. R. M. Pashley and J. N. Israelachvili, 'Molecular layering of water in thin films between mica surfaces and its relation to hydration forces', *J. Colloid Interface Sci.*, **84**, 511–523 (1984).
6. F. T. Madsen and M. Müller-Vonmoos, 'Swelling pressure calculated from mineralogical properties of a Jurassic opalinum shale, Switzerland', *Clays and Clay Minerals*, **33**, 501–509 (1985).
7. R. M. Quigley, F. Fernandez and R. K. Rowe, 'Clayey barrier assessment for impoundment of domestic waste leachate (Southern Ontario) including clay-leachate compatibility of hydraulic conductivity testing', *Can. Geotech. J.*, **25**, 574–581 (1988).
8. R. L. Kranz, D. L. Bish and J. D. Blacic, 'Hydration and dehydration of zeolitic tuff from Yucca Mountain, Nevada', *Geophys. Res. Lett.*, **16**, 1113–1116 (1989).
9. J. D. Blacic, 'Hydration swelling effects on time-dependent deformation of zeolitized tuff', *J. Geophys. Res.*, **98**, 15,909–15,917 (1993).
10. E. Fjær, R. M. Holt, P. Horsrud, A. M. Raaen and R. Risnes, *Petroleum Related Rock Mechanics*, Elsevier, Amsterdam, 1992.
11. A. H. Hale, F. K. Mody and D. P. Salisbury, 'Experimental investigation of the influence of chemical potential on wellbore stability', Paper SPE/IADC 23885 presented at the 1992 IADC/SPE Conf. New Orleans, 18–21 February.
12. G. M. Bol, S. W. Wong, C. J. Davidson and D. C. Woodland, 'Borehole stability in shales', *SPE J. Drilling Completion*, SPE paper 24975, June 1994.

13. W. K. Heidug, 'A thermodynamic theory of fluid-infiltrated porous media undergoing large deformations and changes of phase, Ph.D. Dissertation, Brown University, Providence, RI, 1985.
14. T. A. Hueckel, 'Water–mineral interaction in hygromechanics of clays exposed to environmental loads: a mixture-theory approach', *Can. Geotech. J.*, **29**, 1071–1086 (1991).
15. T. S. Karalis 'Thermodynamics of soils swelling nonhydrostatically', in T. S. Karalis (ed.), *Mechanics of Swelling—From Clay to Living Cells and Tissues*, NATO ASI Series, Springer, Berlin, 1991.
16. V. C. Mow, W. M. Lai and J. S. Hou, 'Triphasic theory for swelling properties of hydrated charged soft biological tissues, *Appl. Mech. Rev.*, **43**, S134–S141 (1990).
17. H. Snijders, J. Huyghe, P. Willems, M. Drost, J. Janseen and A. Hudson, 'A mixture theory approach to the mechanics of human intervertebral disc', in T. S. Karalis (ed.), *Mechanics of Swelling—From Clay to Living Cells and Tissues*, NATO ASI Series, Springer, Berlin, 1991.
18. S. L. Passman, J. W. Nunziato and E. K. Walsh, 'A theory of multiphase mixtures', Appendix to Lecture 5, in C. Truesdell (ed.), *Rational Thermodynamics*, 2nd edn, Springer, New York, 1984.
19. M. Biot, 'General theory of three-dimensional consolidation', *J. Appl. Mech. ASME*, **12**, 15–164 (1941).
20. J. D. Sherwood, 'Biot poroelasticity of a chemically active shale', *Proc. R. Soc. London A*, **440**, 365–377 (1993).
21 S. W. Wong and W. K. Heidug, 'Borehole stability in shales: a constitutive model for the mechanical and chemical effects of drilling fluid invasion', Paper SPE 28059 presented at the 1994 SPE/ISRM Rock Mechanics in Petroleum Engineering Conf., Delft, The Netherlands, 29–31 August.
22. R. Haase, *Elektrochemie I: Thermodynamik elektrochemischer Systeme*, Steinkopff Verlag, Darmstadt, 1986.
23. F. K. Lehner, 'A derivation of the field equations of slow viscous flow through a porous medium', *I&C Fundamentals*, **18**, 41–45 (1979).
24. A. Katachalsky and P. F. Curran, *Nonequilibrium Thermodynamics in Biophysics*, Harvard University Press, Cambridge, MA; 1965.
25. R. Haase, *Thermodynamics of Irreversible Processes*, Dover, New York, 1990; translated from the German *Thermodynamik der irreversiblen Prozesse*, Steinkopff Verlag, Darmstadt, 1963.
26. S. R. de Groot and P. Mazur, *Non-Equilibrium Thermodynamics*, Dover, New York, 1984; reprint of the original edition published by North-Holland, Amsterdam, 1962.
27. C. Truesdell, *Rational Thermodynamics*, 2nd edn, Springer, New York, 1984.
28. E. A. Mason, R. P. Wendt and E. H. Bresler, 'Test of the Onsager relation for ideal gas transport in membranes', *Faraday Trans. II*, **68**, 1938–1959 (1972).
29. E. L. Cussler, *Diffusion–Mass Transfer in Fluid Systems*, Cambridge University Press, Cambridge, 1992.
30. O. Kedem and A. Katchalsky, 'Thermodynamic analysis of the permeability of biological membranes to non-electrolytes', *Biochim. Biophys. Acta*, **27**, 229–246 (1958).
31. A. J. Staverman, 'The theory of measurement of osmotic pressure, *RECUEIL*, **70**, 344–352 (1951).
32. F. K. Mody and A. H. Hale, 'A borehole stability model to couple the mechanics and chemistry of drilling fluid shale interaction', Paper SPE/IADC 25728 presented at the 1993 SPE/IADC Drilling Conf., Amsterdam, 23–25 February.
33. E. von Oort, 'A novel technique for the investigation of drilling fluid induced borehole instability in shales', Paper SPE/ISRM 28064 presented at the 1994 SPE/ISRM Rock Mechanics in Petroleum Engineering Conf., Delft, 29–31 August.
34. R. P. Steiger, 'Advanced triaxial swelling tests on preserved shale cores', *Int. J. Rock Mech. Min. Sci. Geomech. Abstr.*, **30**, 681–685 (1993).
35. P. S. B. Colback and B. L. Wiid, 'The influence of moisture content on the compressive strength of rock', *Proc. 3rd Rock Mechanics Symp.*, Canada Department of Mines and Technical Surveys, Toronto, 1965, pp. 65–83.
36. T. A. Hueckel, 'Strain and contamination history dependence in chemo-plasticity of clays subjected to environmental loads', *Proc. 5th Int. Symp. on Numerical Models in Geomechanics*—NUMOG V, Balkema, Rotterdam, 1995, pp. 329–336.
37. C. Truesdell and R. A. Toupin, 'The classical field theories, in S. Flügge (ed.), *Handbuch der Physik*, Vol III/1, Springer, Berlin, 1960, pp. 226–858.
38. G. J. van Wylen and R. E. Sonntag, *Fundamentals of Classical Thermodynamics*, 2nd edn, Wiley, New York, 1976.
39. J. Kestin, *A Course in Thermodynamics, Vol. I*, revised printing, McGraw-Hill, New York, 1979.
40. A. Nur and J. D. Byerlee, 'An exact effective stress law for elastic deformation of rocks with fluids', *J. Geophys. Res.*, **76**, 6414–6419 (1971).
41. J. R. Rice and M. P. Cleary, 'Some basic stress diffusion solutions for fluid-saturated elastic porous media with compressible constitutents', *Rev. Geophys. Space Phys.*, **14**, 227–241 (1976).
42. P. S. Huyakorn and G. F. Pinder, *Computational Methods in Subsurface Flow*, Academic Press, New York; 1983.
43. R. W. Lewis and B. A. Schrefler, *The Finite-Element Method in Deformation and Consolidation of Porous Media*, Wiley, New York, 1987.
44. I. M. Smith and D. V. Griffiths, *Programming the Finite-Element Method*, Wiley, Chichester, 1988.
45. M. A. Murad and A. F. Loula, On stability and convergence of finite element approximations of Biot's consolidation theory, *Int. J. Numer. Methods in Engng.*, **37**, 645–667 (1994).
46. M. A. Reed, 'An investigation of numerical errors in the analysis of consolidation by finite elements', *Int. J. Numer. Anal. Methods Geomech.*, **8**, 243–257 (1984).